CALCULATION OF THE OVERLAP ANGLE IN SLIP ENERGY RECOVERY DRIVES USING a d,q/abc MODEL

E. Akpinar,MIEEE P. Pillay,MIEEE A. Ersak*,MIEEE

Department of Electrical Engineering
University of New orleans, LA70148
New Orleans, USA

*Department of Electrical and Electronics
Engineering, Middle East Technical University
Ankara, Turkey

Keywords: Induction Motor, Slip Energy, Overlap Angle.

ABSTRACT

In this paper, a closed-form expression to estimate the overlap angle in a slip energy recovery system is presented. The prediction of the overlap angle is important in the case of doubly-fed induction motor drives, because of its influence on speed and torque. A closed-form expression is derived using a hybrid model of the induction motor and a dynamic model of the rotor rectifier. The ripple content of the dc link current and the inverter input voltage are neglected. The predicted results obtained using the closed form expression are verified experimentally.

1. INTRODUCTION

The effects of the overlap angle on the rectifier output voltage in a slip energy recovery drive system shown in figure 1 [1] can be considerable. Neglect of the overlap can lead to a 15% or larger error in the calculation of the torque. A control strategy for maximizing the amount of the slip energy recovered from the rotor is also affected by the knowledge of the overlap angle. In normal operation, the overlap angle is less than 60° [2]. Overlap in a three phase bridge rectifier occurs when three devices in the three-phase bridge rectifier conduct simultaneously, one from the common anode group and two from the common cathode group, or vice versa. The overlap angle is the overlap period multiplied by the source frequency.

The effect of the overlap angle on the drive performance under steady-state operating conditions has been considered [2] using a numerical integration technique. The estimation of the overlap angle based on the equivalent circuit neglects the stator and the rotor flux changes [3], and the effect of mutual inductance [4]. Some efforts to predict the overlap angle are based on the d,q model of induction machines and take both the stator and rotor electrical transients into account [2,5]. There are still ongoing discussions on whether the overlap angle depends on the speed or not. With a constant dc link current under steady state operating conditions, the effect of slip variation on the overlap angle has been noted [2,5], yet [6] states that the overlap angle might be independent of the rotor speed.

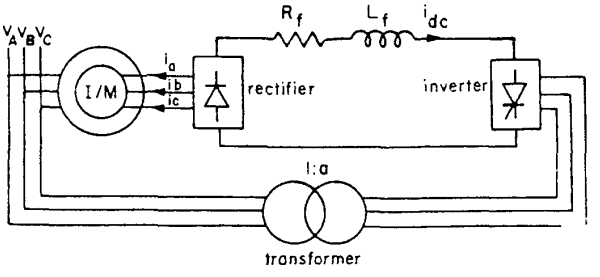

Fig. 1. Schematic representation of a slip energy recovery system

All previous work used the average value of the dc link current, with the rotor speed and machine parameters being input variables in estimating the overlap angle under steady state operating conditions. They also assume that the rotor terminal voltage is always sinusoidal, and that the dc link current does not contain ripple.

In this paper, a closed-form expression is obtained for the estimation of the overlap angle, based on a transient model developed for the slip energy recovery system [1]. The rotor terminal voltage is assumed to maintain its original non sinusoidal waveshape, hence one more variable, namely the mean output voltage of the recovery inverter, is included in the closed form expression to predict the overlap angle. The dc link current ripple is however neglected.

2. MATHEMATICAL MODEL OF THE INDUCTION MACHINE

A hybrid model which retains the actual rotor phase variables but transforms the stator only, has been proposed to examine the transient [1] and steady state [7] performance of a slip energy drive system. In the model

92 SM 543-9 EC A paper recommended and approved by the IEEE Electric Machinery Committee of the IEEE Power Engineering Society for presentation at the IEEE/PES 1992 Summer Meeting, Seattle, WA, July 12-16, 1992. Manuscript submitted January 30, 1992; made available for printing May 15, 1992.

used, it is assumed that the d' axis coincides with the fundamental component of the phase A of the rotor while the q' axis leads the d' by 90° (electrical). The non-linear differential equations of the hybrid model for the induction machine are as follows [1];

$$\begin{bmatrix} v_d' \\ v_q' \\ v_a \\ v_b \\ v_c \end{bmatrix} = \begin{bmatrix} R_s+L_s p & -w_e L_s & Mp & -(Mp + \sqrt{3}Mw_e)/2 & (-Mp + \sqrt{3}Mw_e)/2 \\ w_e L_s & R_s+L_s p & Mw_e & (\sqrt{3}Mp - w_e M)/2 & -(\sqrt{3}Mp + w_e M)/2 \\ Mp & 0 & R_r+L_r p & M_r p & M_r p \\ -Mp/2 & \sqrt{3}Mp/2 & M_r p & R_r+L_r p & M_r p \\ -Mp/2 & -\sqrt{3}Mp/2 & M_r p & M_r p & R_r+L_r p \end{bmatrix} \begin{bmatrix} i_d' \\ i_q' \\ i_a \\ i_b \\ i_c \end{bmatrix} \quad (1)$$

where

$$v_d' = \sqrt{(3/2)} V_m \text{ Cos } (w_s t-\theta)$$

$$v_q' = \sqrt{(3/2)} V_m \text{ Sin } (w_s t-\theta) \quad (2)$$

$w_s = 2\pi f$

and v_a, v_b, v_c are the rotor line to neutral voltages.

3. RECTIFIER MODEL

The operation of the rectifier in the rotor of the induction motor is complicated by the excessive complex source impedance of the motor. The operation of the diode bridge rectifier can be analyzed using four different modes [8,9], as a result of the overlap angle. In this work, it has been assumed that no more than three diodes ever conduct simultaneously. The instantaneous rotor phase voltages and the rotor phase currents are given in Fig.2. While sinusoidal voltages are shown in Fig. 2, the actual logic implemented is based on the true nonsinusoidal voltages that exist in the rotor when connected to a diode bridge rectifier. Fig.3 is an effective equivalent circuit of the rotor rectifier fed with the rotor phase voltages v_a, v_b and v_c. Included are the link resistance and the average value of the inverter voltage, V_i. Referring to Table 1, in conduction sequence '1', there are only two elements, D1 and D6 conducting. In sequence '2', however, there are three diodes D1, D2 and D6 conducting, and the first two carry the same dc output current in total. The current in rotor phase 'a' commutates to phase 'b' causing the overlap phenomenon. Table 1 summarizes twelve conduction sequences resulting from the operation of the rectifier and the constraints applied to the circuit as a result of the conduction sequences of the diodes. The governing voltage equations in the system for all 12 possible conduction sequences are summarized in Table 2 in accordance with the associated dc link current shown in Table 1. The mean input voltage, V_i of the inverter is in opposite polarity in the first six equations to that in the last six equations, which are otherwise identical. Only three conduction sequences of the six, namely 2, 4 and 6 relate to the rectifier operation during overlap.

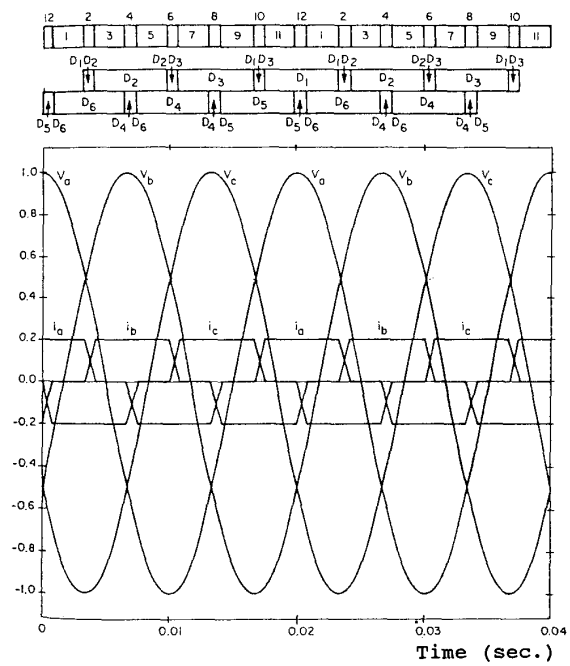

Fig. 2. Conduction sequence of the diodes in the bridge rectifier based on the rotor phase voltages and currents

The submatrices that correspond to each conduction sequence has been published previously [1]. They are basically derived by imposing the constraints in Table 2 to the general model of the machine given in (1). In order to derive the closed-form expression for the overlap angle, it is necessary to use equation (1) in state-space form, subject to the constraints of a given conduction sequence. The state-space form of equation (1) has the inverse of an inductance matrix, with several entries in that matrix being zero, when equation (1) is subjected to the constraints of conduction sequence 6. Conduction sequence 6 is therefore chosen for derivation of the overlap angle, μ.

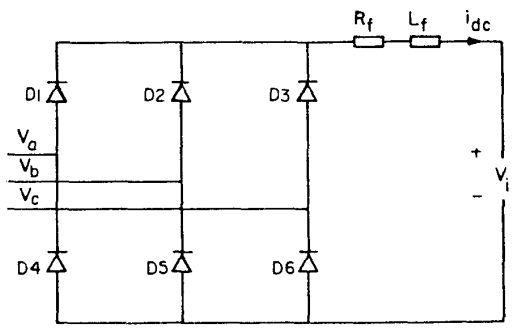

Fig. 3. Rotor rectifier

Table 1 *

Conduct. Seq.	Conduct. Diodes	Phases in Overlap	Rotor Phase Constraints	Dc Link Current Idc
1	1,6	-	$i_b = 0$	$-i_a$
2	1,6,2	a,b	$v_a - v_b = 0$	i_c
3	6,2	-	$i_a = 0$	i_c
4	6,2,4	-c,-a	$v_a - v_c = 0$	$-i_b$
5	2,4	-	$i_c = 0$	i_a
6	2,4,3	b,c	$v_b - v_c = 0$	i_a
7	4,3	-	$i_b = 0$	i_a
8	4,3,5	-a,-b	$v_a - v_b = 0$	$-i_c$
9	3,5	-	$i_a = 0$	$-i_c$
10	3,5,1	c,a	$v_a - v_c = 0$	i_b
11	5,1	-	$i_c = 0$	$-i_a$
12	5,1,6	-b,-c	$v_b - v_c = 0$	$-i_a$

* those underlined are the commutating diodes

Table 2

Conduction Sequences	System Voltage Equations
1	$v_a - v_c = V_l - (R_f + L_f p)\, i_a$
2	$v_a - v_c = V_l + (R_f + L_f p)\, i_c$
3	$v_b - v_c = V_l + (R_f + L_f p)\, i_c$
4	$v_b - v_c = V_l - (R_f + L_f p)\, i_b$
5	$v_b - v_a = V_l + (R_f + L_f p)\, i_a$
6	$v_b - v_a = V_l + (R_f + L_f p)\, i_a$
7	$v_a - v_c = -V_l - (R_f + L_f p)\, i_a$
8	$v_a - v_c = -V_l + (R_f + L_f p)\, i_c$
9	$v_b - v_c = -V_l + (R_f + L_f p)\, i_c$
10	$v_b - v_c = -V_l - (R_f + L_f p)\, i_b$
11	$v_b - v_a = -V_l + (R_f + L_f p)\, i_a$
12	$v_b - v_b = -V_l + (R_f + L_f p)\, i_a$

4. OVERLAP PERIOD

Consider conduction sequence 6 in which rotor phases b and c are in parallel through the conducting diodes D2 and D3 due to overlap, and the rotor circuit connections take the form shown in Fig.4. The dc link current, I_{dc} commutates from rotor phase b to c, and hence the sum of these two currents is $-I_{dc}$ in this conduction sequence. The rotor phase currents at any instant satisfy the condition ($i_a + i_b + i_c = 0$), and therefore the dc link current is equal to $+i_a$ as shown in Table 1.

Let the rotor phase voltage equations defined in (1) for conduction sequence 6 be rewritten as;

$$v_a = Mpi_d' + R_r i_a + L_{rr} p i_a \qquad (3)$$

$$v_b = (-1/2)Mpi_d' + (\sqrt{3}/2)Mpi_q' + R_r i_b + L_{rr} p i_b$$

$$v_c = (-1/2)Mpi_d' - (\sqrt{3}/2)Mpi_q' + R_r i_c + L_{rr} p i_c$$

where $L_{rr} = L_r - M_r$. Substituting v_b and v_c of (3) into the constraint equation for conduction sequence 6 given in Table 1, i_b and i_c are then related to each other through the dc link current, I_{dc}. One of these two currents may be eliminated from the voltage equations; i_b is eliminated in this case. Also, I_{dc} in the rotor voltage equations is replaced by i_a.

The stator equations in (1) are also modified similarly, so that one of the commutating currents will be left in the voltage equations as given in (4) for conduction sequence 6. The associated voltage constraint equation gives the last row entries in (4). The mesh equation, which may be written around the loop formed by the rotor phase "a" winding, D1, dc link, the inverter, D2 and the rotor phase "c" winding yields the third row entries of (4).

$$\begin{bmatrix} v_d \\ v_q \\ V_l \\ 0 \end{bmatrix} = \begin{bmatrix} R_s + L_s p & -w_e L_s & \{(3/2)Mp + (\sqrt{3}/2)Mw_e\} & \sqrt{3}Mw_e \\ w_e L_s & R_s + L_s p & \{(3/2)Mw_e - (\sqrt{3}/2)Mp\} & -\sqrt{3}Mp \\ -(3/2)Mp & (\sqrt{3}/2)MP & -2R_r - R_f - (2L_{rr} + L_f)p & -R_r - L_{rr} p \\ 0 & -\sqrt{3}Mp & R_r + L_{rr} p & 2R_r + 2L_{rr} p \end{bmatrix} \begin{bmatrix} i_d' \\ i_q' \\ i_a \\ i_c \end{bmatrix} \qquad (4)$$

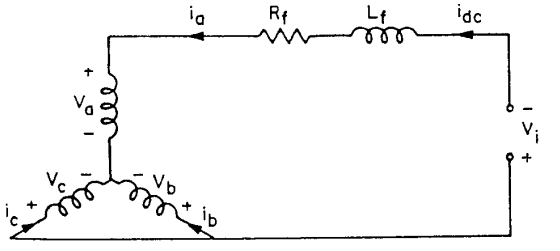

Fig.4 Circuital diagram for conduction sequence 6

From (4) the general form of the expression for the state variable vector, which consists of two stator and two rotor currents is arranged as:

$$pi = [L^{-1}]\ [v - Ri] = [L^{-1}]A \qquad (5)$$

Considering the specific case for conduction sequence 6, derivatives of the rotor phase currents i_a and i_c can be obtained from (5) as:

$$pi_a = (-L_{13}A_1 + 2L_{34}A_3 + L_{34}A_4)/det[L] \qquad (6)$$

$$pi_c = (L_{13}A_1/2 + L_{42}A_2 - L_{34}A_3 + L_{44}A_4)/det[L] \qquad (7)$$

where

$$L_{13} = -3ML_{rr}L_s + 9M^3/2$$

$$L_{34} = L_s^2L_{rr} - 3M^2L_s/2$$

$$L_{42} = -3\sqrt{3}ML_{rr}L_s + 9\sqrt{3}M^3/4$$

$$L_{44} = -2L_{rr}L_s^2 + 3M^2L_s$$

$$det[L] = -3L_{rr}^2L_s^2 + 9M^2L_rL_s - 27M^3/4$$

and A_i $i=1\ldots4$ is the element of the vector A, as;

$$A_1 = V_sCos(w_st-\theta) - R_si_d + w_eL_si_q' - (\sqrt{3}/2)w_eMi_a - \sqrt{3}w_eMi_c\ ,$$

$$A_2 = V_sSin(w_st-\theta) - w_eL_si_d' - R_si_q' - (3/2)Mw_ei_a, \qquad (8)$$

$$A_3 = V_1 + (2R_r + R_f)i_a + R_ri_c\ ,$$

$$A_4 = -R_ri_a - 2R_ri_c\ ,$$

Assuming that the ripple on the dc link current I_{dc} (= i_a) is negligibly small, i.e., $pi_a = 0$, Eqns.(6) and (7) can be solved for A_1 to yield;

$$pi_c = ((L_{34}/2 + L_{44})A_4 + L_{42}A_2)/det[L] \qquad (9)$$

The solution of (9) requires knowledge of the initial conditions of the stator currents. Expressions for pi_d' and pi_q' are derived from the last two rows of (4) as;

$$pi_d' = -(2/3M)(V_1 + R_fi_a + (3/2)R_ri_a) \qquad (10)$$

$$pi_q' = (1/\sqrt{3}M)(R_ri_a + 2i_cR_r + 2L_{rr}pi_c) \qquad (11)$$

The second derivative of i_c is found after substituting (10) and (11) into (9):

$$p(pi_c) = Dpi_c + Ei_c + F + Gcos(sw_st) \qquad (12)$$

where $V_s = \sqrt{(3/2)}V_m$, $s = (w_s - w_e)/w_s$ in which $w_et = \theta$, and

$$D = \{-2R_r(L_{44}+L_{34}/2) - 2L_{42}R_sL_{rr}/(\sqrt{3}M)\}/det[L]$$

$$E = \{-2L_{42}R_sR_r/(\sqrt{3}M)\}/det[L]$$

$$F = sw_sV_sL_{42}/det[L]$$

$$G = \{(2L_{42}w_eL_s(R_f + 3R_r/2)/(3M) - L_{42}R_sR_r/(\sqrt{3}M))I_{dc} + (2L_{42}w_eL_s/3M)V_1\}/detL$$

The voltage v_d' is in phase with the fundamental component of the rotor phase voltage "a" in the hybrid reference frame, and hence

$$sw_st = w_st - \theta\ .$$

The solution of (12) can be carried out by using the final values of the rotor currents in conduction sequence 5 as the initial values in conduction sequence 6 which are;

$$i_a(t_o) = -i_b(t_o) = I_{dc},$$

$$i_c(t_o) = 0$$

$$pi_c(t_o) = 0 \qquad (13)$$

at t_o, the beginning of the overlap period. The final values of the rotor currents at t_1, the end of the overlap period, are:

$$i_a(t_1) = I_{dc},$$

$$i_b(t_1) = 0,$$

$$i_c(t_1) = -I_{dc} \qquad (14)$$

which are also the initial values for the rotor currents in state 7. The time elapsed in commutating the current from phase "b" to "c" in state 6 is then (t_1-t_o). The solution for (12) is found, in accordance with these initial and final values of the respective phase currents, as;

$$i_c(t_1) = \alpha_o + \alpha_1exp((\pi+\mu)r_1/(sw_s)) + \alpha_2exp((\pi+\mu)r_2/(sw_s)) - \alpha_3Cos\mu - \alpha_4sin\mu = -I_{dc} \qquad (15)$$

where

$$\alpha_o = \{((2L_{42}w_eL_s(R_f + 3R_r/2))/3M - L_{42}R_sR_r/\sqrt{3}M)I_{dc} + 2L_{42}w_eL_sV_1/3M\}/(2L_{42}R_sR_r/\sqrt{3}M)$$

$$\alpha_1 = \frac{r_2(\alpha_5 - \alpha_0) - sw_s\alpha_6}{r_2 - r_1}\ exp(-r_1\pi/(sw_s))$$

$$\alpha_2 = \frac{1}{H}(-r_1(\alpha_5 - \alpha_0) + sw_s\alpha_6)\ exp(r_1\pi/(sw_s))$$

$$\alpha_3 = -\frac{F(E + (sw_s)^2)}{(E + (sw_s)^2)^2 + (Dsw_s)^2}\ ,$$

$$\alpha_4 = -\frac{F\ D\ sw_s}{(E + (sw_s)^2)^2 + (Dsw_s)^2}\ ,$$

$$r_1 = (D + \sqrt{(D^2 + 4E)})/2\ ,$$

$$r_2 = (D - \sqrt{(D^2 + 4E)})/2\ ,$$

$$H = (r_2-r_1)\ exp((r_1 + r_2)\pi/(sw_s))\ .$$

5. RESULTS

The results presented in this section are carried out on a slip energy recovery system consisting of a 3 phase, 380 V, 3.5 kW, 8.1 A, 50 Hz, 4-pole, slip ring induction machine having the following parameters referred to the rotor side;

R_s = 0.144 ohms, L_s = 0.065 H,

R_f = 1.49 ohms R_r = 0.2 ohms,

L_{rr} = 0.065 H, M = 0.0522 H

Figure 5 shows the predicted and measured overlap angle variations with the rotor speed. The experimental results in figure 5 are obtained under closed loop current and speed control of a slip energy recovery system. The slip, inverter input voltage and dc link current are controlled in order to obtain the data for figure 5. The process is repeated for different commanded values of speed to collect a set of data. Equation (15) is used to predict the overlap angle. This equation is a function of the machine parameters (R_s, L_s, R_r, L_{rr}, M), filter resistance R_f, infinite bus voltage V_s, slip s, average value of dc link current I_{dc} and average value of the inverter input voltage V_I. The predicted values of the overlap angle are obtained by keeping the machine parameters and infinite bus voltage constant. The experimental measurements of the rotor speed, dc link current and inverter input voltage are used in (15) to predict the overlap angle.

The overlap angle is measured over a range of loads and speeds. The results show that the overlap angle and the rotor speed are interrelated. i.e, there is an increase in the overlap angle as the speed increases. This is caused by the source resistance. The magnitude of both the rotor leakage reactance and the rotor voltage decreases with the reduction in rotor frequency. Hence in the absence of resistance, the overlap angle would remain constant with a reduction in slip (and hence rotor frequency) since the motor reactance and rotor open circuit voltage appear as a ratio in the overlap equation. However, the voltage drop on the rotor resistance remains constant for constant current at a given temperature. Hence the relative voltage drop across the source resistance increases as the slip reduces causing the effective source voltage to be reduced beyond that dictated by the reduction in rotor frequency. Also, the overlap angle increases as the dc link current increases. There is a small difference between the predicted and measured overlap angle, since the derivation of the closed-form expression for the overlap angle prediction is based on assuming a smooth dc link current.

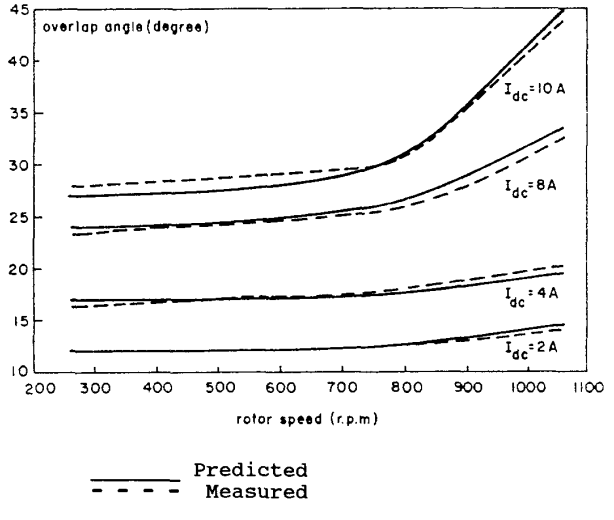

Fig. 5. Measured and predicted overlap angle

Table 3 presents the experimental results for the variation of the inverter input voltage with respect to the dc link current and rotor speed. It can be observed that the inverter input voltage is not unique at a particular value of rotor speed, it also depends on the magnitude of dc link current.

Table 3.

n_r(r.p.m)	I_{dc}(A)	V_I(V)	n_r	I_{dc}	V_I
257	2	160	257	8	146
509	2	130	509	8	116
793	2	90	793	8	78
1061	2	56	1061	8	46
257	4	155	257	10	143
509	4	124	509	10	112
793	4	84	793	10	76
1061	4	50	1061	10	44

6. CONCLUSION

This paper has presented an analytical technique for the calculation of overlap angle on the rectifier output voltage in slip energy recovery induction motor drives; the machine may be operated as a motor or generator. The rotor voltages are not assumed to be sinusoidal, leading to a more accurate result than [2]. The rotor current waveform may also be determined if it is desired, using equation (12) which can be used for an harmonic analysis of the current waveforms. This technique is only possible because of the hybrid dq/abc model used here which has a time invariant state space form at constant speed. A closed form solution is not possible if a full ABC/abc model is used, thus requiring numerical integration for solution.

Acknowledgements:

E. Akpinar would like to thank the British Council for funding his research at the University of Newcastle upon Tyne in UK and the Middle East Technical University (METU) in Turkey for funding his research at METU under contract no AFP-90-03-01-02. He would also like to thank EPRI and Entergy Corporation in the USA.

P. Pillay would like to thank EPRI, Entergy, Mobil Oil Chalmette Refinery, Louisiana Power and Light Co. and CLECO for funding his research.

REFERENCES

[1] E. Akpinar and P. Pillay, "Modelling and Performance of Slip Energy Recovery Induction Motor Drives" , IEEE Trans., Energy Conversion, Vol.5, No.1, March 1990, pp. 203-210.

[2] Salameh, Z.M., Kazda, Z.F., "Analysis of the Double Output Induction Generator Using Direct Three-Phase Model Part I- Commutation Angle Analysis", IEEE Trans., Energy Conversion, Vol. EC-2, June 1987, pp. 175-181.

[3] Al Zahawi, B.A.T., Jones, B.l., Drury W., "Effect of Rotor Rectifier on Motor Performance in Slip Recovery Drives", Can. Elect. Eng. J., Vol. 12, No. 1, 1987, pp.24-32.

[4] Lavi, A., Polge, R.J. "Induction Motor Speed Control with Static Inverter in the Rotor " IEEE Trans., Power Apparatus and Systems, Vo. PAS-85, No.1, January 1966, pp. 76-84.

[5] Surendran, K., Subrahmanyam, V., "Analysis of a Variable Speed Induction Motor Drive Employing Static Slip Energy Recovery Scheme", ICEM, 1986, pp. 889-891.

[6] Bland, R.J., Hancock, N.N., Whitehead R.W., "Considerations Concerning a Modified Kramer Drives", Proc. IEE, Vol. 110, No. 12, December 1963, pp. 2228-2232.

[7] J.E. Brown, W. Drury, B.L. Jones and P. Vas, "Analysis of the Periodic Transient States of a Static Kramer Drive", Proc IEE, Vol.133, Pt.B, No. 1, pp 21-30.

[8] B.D. Bedford, R.G. Hoft, "Principles of Inverter Circuits", John Wiley and Sons, Inc., 1974.

[9] V. H. Jones and W.J. Bomwick, "Three Phase Bridge Rectifiers With Complex Source Impedance", Proc. IEE Trans, Vol. 122, No. 6 June 1975, pp. 630-636.

LIST OF SYMBOLS

a	= Turns ratio of the transformer
i_a, i_b, i_c	= Rotor phase a, b, c currents respectively, A.
i_{dc}	= dc link current, A.
i_d', i_q'	= d', q' axis stator currents in hybrid reference frame, A.
I_{dc}	= Mean value of the dc link current, A.
f	= Frequency of the infinite bus voltage, Hz.
L_f	= Link inductor inductance, H.
L_{rr}	= Self inductance of one phase of a three phase rotor winding, H.
L_s	= Self inductance of one phase of a three phase stator winding, H.
L_r'	= $L_r + M_r'$
M	= Maximum value of the mutual inductance between a stator and a rotor phase winding, H.
M_r'	= Mutual inductance between two rotor phases, H.
p	= d/dt
R_f	= Link inductor resistance, Ω.
R_r	= Per phase resistance of rotor windings, Ω.
R_s	= Per phase resistance of stator windings, Ω.
v_a, v_b, v_c	= Rotor terminal voltages of phase a, b, c,V.
v_i	= Instantaneous voltage at the inverter dc terminal, V.
V_i	= Mean value of the inverter input voltage, V.
V_m	= Peak value of the line to neutral voltage at infinite bus, V.
v_d',v_q'	= d', q' axis stator voltages in hybrid reference frame, V.
w_e	= $d\theta/dt$
w_s	= Angular frequency of supply, rad/s.
θ	= Elect. angle between stator and rotor phase A, rad.
μ	= Overlap angle, rad.

Eyup Akpinar (S'87-M'91) obtained the B.Sc and M.Sc and Ph.D degrees in electrical engineering from the Middle East Technical University (METU), Ankara, Turkey in 1981, 1984 and 1991 respectively. His M.Sc thesis was concerned with the optimum design of multi-pole synchronous generators. He was awarded a scholarship by the British Council to do part of his Ph.D thesis at the University of Newcastle upon Tyne in United Kingdom (UK).

He is now on leave from METU and doing postdoctoral research at the University of New Orleans. He is a member of the Power Engineering, Industry Applications, Power Electronics and Industrial Electronics Societies of the IEEE. He is also a member of the Chamber of Electrical Engineers of Turkey. His research interests include the control, modeling and design of electrical machinery and drives.

Pragasen Pillay (S'84-M'87) received the B. Eng, M.Sc(Eng), and Ph.D degrees, all in electrical engineering. The Ph.D degree was obtained at the Virginia Polytechnic Institute and State University, Blacksburg, while funded by a Fulbright Scholarship.

He is currently with the Department of Electrical Engineering, University of New Orleans. His research interests are in modeling, control, and design of electric motor drive systems.

Dr. Pillay is a past recipient of an IEEE prize award paper. He is a member of the Industry Applications, Industrial Electronics, and Power Engineering Societies of the IEEE and a member of the Industrial Drives, Electric Machines and Education Committees of the Industry Applications Society. He is also a Member of the Institution of Electrical Engineers, England, a Chartered Electrical Engineer and a member of the Greek Honor Society, Phi-Kappa-Phi.

Aydin Ersak has the Bachelor's, Master's and Ph.D degrees all in Electrical Engineering. All degrees were obtained from the Middle East Technical University, Ankara, Turkey. He is with the Department of Electrical and Electronics Engineering, Middle East Technical University, Turkey.

His research interests include the control and design of electrical drives and power converters. He is a member of IEEE.